MATHEMATICAL MODELLING TOOLS FOR THE OPTIMISATION OF DIRECT SMELTING PROCESSES

M. P. Davis[1], K. Pericleous[2], M. P. Schwarz[3] and M. Cross[2]
[1]RTZ-CRA Research and Technology, Bentley, Western Australia
[2]Centre for Numerical Modelling & Process Analysis, The University of Greenwich, London
[3]CSIRO Division of Minerals, Clayton, Victoria

ABSTRACT

Direct smelting operations involve the strong interaction of a wide range of complex physico-chemical processes. Moreover, for such processes to be efficient, these interactions have to be optimised to yield the desired set of chemical reactions and exchanges of heat and mass amongst the variety of gaseous, liquid and solid phases. This paper focuses upon a consideration of Computational Fluid Dynamics (CFD) based models developed to represent the HIsmelt® direct smelting process. The models are extremely sophisticated and at every stage have challenged the limits of CFD technology, as well as the adequacy of constitutive sub-models to represent the chemical reaction/combustion phenomena. From an unprecedented synergy amongst process metallurgists, experimental scientists and CFD modellers, sophisticated, comprehensive and well validated models of the process have evolved. The paper highlights some of the key state-of the-art CFD techniques developed for the models and the role of specially designed experiments in parameter estimation and validation against plant measurements.

NOMENCLATURE

C_D	drag coefficient
g	gravitational constant
m_d	droplet mass
n	number of phases
N_d	number of droplets per unit volume
r	droplet radius
R_i	volume fraction of i^{th} phase
S_ϕ	source term for variable ϕ
S_{mi}	mass source term of i^{th} phase
t	time
u_d	droplet velocity component
u_g	gas velocity component
$\vec{U}$	gas vector velocity
$\vec{U}_i$	gas vector velocity of i^{th} phase
ϕ	variable solved for
Γ_ϕ	exchange coefficient
ρ, ρ_g	gas density
ρ_i	density of i^{th} phase

1. INTRODUCTION

For a variety of reasons a clear market demand is emerging for reduced iron as the raw material to replace iron ore. It may be argued that the ideal process to satisfy this demand should take ore as fines, and coal of a wide variety of types. It should yield a hot metal product that may be immediately refined to steel and formed into products. Moreover, the ore should not require pre-treatment and the coal type should not be restricted to coking coal. For such a process to be successful it must involve relatively low capital and operating costs as well as being environmentally sound.

1.1 History of the HIsmelt® Process

The HIsmelt Process is the result of a substantial effort, primarily supported by CRA, to develop a route which satisfies the above challenges and provides a core technology to meet the needs of the iron ore market as it is transformed into a more value added business in the 21st Century[1-5]. In 1981 CRA recognised the significant potential for developing an intensive coal-based direct smelting operation based upon the K-OBM and KMS steelmaking processes of Klöckner-Werke. These organisations formed a joint venture in 1982 focussed upon the development of a new ironmaking process.

The genesis of the HIsmelt Process was the recognition that oxygen steelmaking, using supplementary coal injection and high post

combustion levels to achieve high scrap melting rates, could be adapted to meet the technical objectives of a competitive iron ore smelting technology. After successfully testing the smelt reduction concept in a 60t OBM converter, a 10t iron bath capacity Small Scale Pilot Plant (SSPP) facility was designed and built at Klöckner's Maxhütte Steelworks in southern Germany. This process operated from 1984 until 1990, when it was decommissioned. CRA took full responsibility for this process in 1986 and from 1989-1994 worked in a joint venture with Midrex Corporation to pursue the development of the next phase of HIsmelt. This involved the development of the HIsmelt Research and Development Facility (HRDF) in Kwinana, Western Australia.

As one might expect the flowsheet utilises a wide range of unit processes. Mathematical modelling has, in fact, been used extensively in the design, control and optimisation phases of each stage of the HIsmelt Process development. An overview of the key aspects of this work has been recorded by Hardie et al[5]. In this paper the key focus will be modelling of the core unit process of HIsmelt - the Smelt Reduction Vessel (SRV). This activity has been underway for some 14 years and, inevitably, what can be described in a paper of this nature is an overview of the work and some indication of its impact upon the process development.

1.2 Smelt Reduction Vessel - the Core of the Process

Smelt reduction processes utilise the heat released by the combustion of carbon and other hydrocarbons in a reactor containing a molten bath, to achieve simultaneous smelting of ore to metal and the formation of a slag phase from the gangue components in the ore, flux and coal. Within the smelt reduction vessel, volatiles in the coal are cracked, carbon is dissolved in the metal, ore is smelted and molten slag formed. Since all these reactions are endothermic, substantial quantities of heat have to be supplied to the metal bath to maintain its temperature. The key to the HIsmelt Process is the generation of high post-combustion in the top space and the efficient transfer of that heat back to the bath to facilitate the smelting of the injected ore.

The core of the HIsmelt Process, the SRV, is shown conceptually in figure 1.

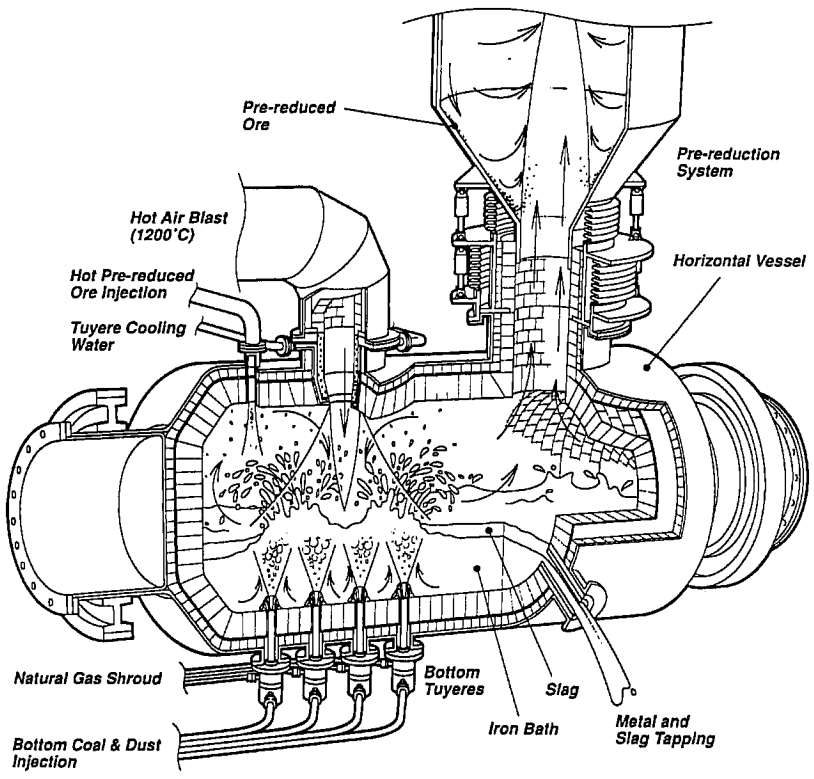

Figure 1. Conceptual HIsmelt smelt reduction vessel.

The main features of the process are:

- injection of coal, ore and fluxes into the vessel;
- the creation of a highly agitated bath; and
- the injection of oxygen as preheated air into the top space.

The injection rates of solids and gases are targeted to produce a top space stoichiometry that enables the heat transfer to the bath to occur very efficiently. Figure 2 illustrates the set of major reactions that occur, together with the broad role of the solid, liquid and gaseous phases. A key factor in the success of the SRV operation is the generation and control of an agitated bath surface, so that an effective interfacial area may be maintained between the top space combustion gases and the molten bath to promote the high rate of heat transfer to the bath.

1.3 Modelling the Smelt Reduction Vessel - Partitioning the Process

In order to make the modelling exercise more tractable, three distinct volumes within the smelting vessel have been identified from the start. These have been named the Bath Zone, the Transition Zone and the Gas Zone (refer to figure 2). Each covers a volume of the vessel where distinctions in the physico-chemical aspects of the process can be made and where these distinctions enable the most efficient utilisation of a particular model concept. As the names suggest, the bath zone is the volume of the converter where the liquid metal and slag form a continuous phase, the gas zone is where the gas phase is continuous, and the transition zone is where the gas phase is continuous but there exists a significant amount of the liquid phase in the form of liquid 'fingers' or droplets.

Upon commencement of the HIsmelt CFD modelling work, the gas continuous volume of the converter was considered to constitute the more straightforward part of the process to simulate as CFD techniques were already established which could handle this class of flow. This modelling work was undertaken by a group of workers, initially at CHAM Ltd, and more recently at RTZ-CRA Research and

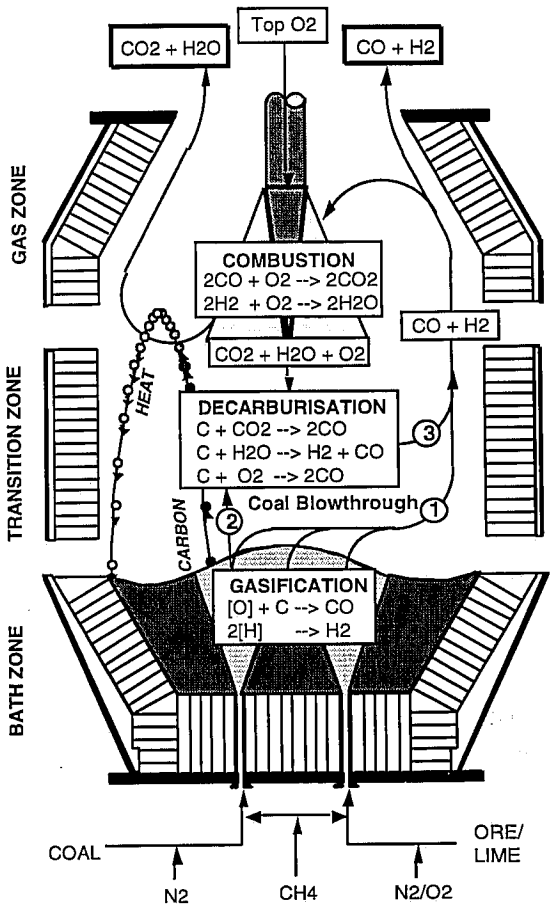

Figure 2. Post combustion stoichiometry.

Technology and the University of Greenwich. The CFD package PHOENICS being used as the framework for the model development.

Due to the high volumes of gas being injected into the metal and slag bath, and the high intensity of the mixing taking place as a result, the modelling of the bath zone was considered to be more problematic as modelling techniques had to be developed which could characterise this part of the process. A more research orientated modelling approach was therefore utilised by workers at the CSIRO who undertook this modelling exercise (also using PHOENICS). The models developed by these two groups of workers have come to be known as the 'bath model' and the 'top space model'.

Splitting the converter volume into two regions is in reality an artificial distinction as there is in fact no distinct boundary in the process. However, it has enabled what would otherwise have been an intractable modelling exercise to

proceed and produce significant benefits for the HIsmelt development team. In the rest of this paper the focus is on the CFD modelling of both the 'top space' and 'bath' models, their development, validation and application in the design and operational optimisation of the HIsmelt Process.

2. TOP SPACE MODELLING OF THE HISMELT PROCESS

Various aspects of the top space model development have already been described[5,6]. The model is in effect a fully three dimensional representation of the liquid and gas flow within the top space together with the associated heat and mass transfer processes. For ease of model formulation and implementation within a CFD framework, the top space model can be considered to consist of five sub-models:

- a turbulent reacting gas space model;
- a Lagrangian particle tracking formulation for the treatment of the liquid phase;
- a model of the heat and mass transfer between the two phases due to combustion;
- a two-phase six-flux radiation model to calculate the radiant fluxes; and
- a specially developed gas turbulence model for regions with high swirl.

Together with the mechanics of specifying the inflow and outflow boundary conditions, and the calculation of cell blockages to model the converter shape, the above sub-models constitute the top space model.

2.1 Conservation Equations

The steady-state turbulent non-isothermal flow in the converter is characterised by the following partial differential equation, which represents in a compact form the transport of a generic conserved variable ϕ under the influence of a source S_ϕ:

$$\nabla\left(\rho\vec{U}\phi - \Gamma_\phi \nabla\phi\right) = S_\phi \qquad (1)$$

The first term in the equation gives transport by convection, whilst the second term represents gradient diffusion, governed by the exchange coefficient Γ_ϕ, which contains laminar and turbulent contributions. Conserved variables for this problem include mass (ϕ = 1), momentum (with ϕ = u, v or w the velocity components in three coordinate directions) and enthalpy ($\phi = h$, which contains sensible heat and heat of reaction contributions). Additional conserved variables represent top-space chemical reactions and turbulence.

The precise form of the source rate term S_ϕ will depend on the equation addressed. In the momentum equations it encompasses the pressure gradient and interface drag forces in the transition zone. In the enthalpy equation it contains radiation contributions, and in the chemical species equations the generation and consumption rates of the reactants.

Equation (1) is discretised by integration on a computational grid using a standard finite-volume procedure. A large number of linear finite-domain equations result from this process that are then solved iteratively in the CFD code PHOENICS. To reduce problems of numerical diffusion a structured cylindrical polar type mesh was used for most SRV simulations. The axis of the mesh was made to coincide with the main jet axis of the top air tuyere. The shape of the vessel was then "carved out" of this mesh using partial cell blockages. These blockages, which are used to modify cell volumes and areas, are also used as porosities to represent the gas volume reduction arising from the presence of the liquid phase within the transition zone.

2.2 Transition Zone

The transition zone region of the converter is assumed to consist of a 'fountain' of droplets ejected into the top space by the highly turbulent motion of the bath caused by the bottom injection processes. In the model the 'bath surface' is assumed to be flat. Both these assumptions are idealisations of reality, since in actual fact there may be no bath surface at all, but rather a well mixed region where fingers or upwellings of the liquid metal and slag exist but are not sufficiently diffuse as to allow for the continuous passage of the top space gases.

Within the CFD field there are two main methods for modelling multiphase processes: the Eulerian-Eulerian approach which assumes the two phases are inter-penetrating continua, each with its own set of momentum equations; and the Lagrangian approach which models the dispersed 'particle' phase by calculating a large number of trajectories for this phase in a Lagrangian frame of reference. As there are within the top space a multitude of droplets of different sizes moving predominantly up and down in a ballistic manner, the Eulerian concept of having a single velocity vector in each computational cell to describe this situation is inappropriate. Hence the Lagrangian approach was chosen to model the liquid phase. So in addition to the continuum equations given in (1), momentum equations of the following form are solved for the droplets:

$$m_d \frac{du_d}{dt} = m_d g - \frac{1}{2}\rho_g \left|u_d - u_g\right|(u_d - u_g) C_D \pi r^2 N_d \qquad (2)$$

Where N_d is the number of droplets per unit volume, m_d their mass and C_d the drag coefficient of a spherical particle. The drag term in the equation reflects the interchange of momentum between gas and droplets. Heat transfer between the gas and droplets is partly represented through a convective term which depends on the Nusselt number. The interphase drag and heat and mass transfer coefficients used are the standard empirical correlations found in the literature[7,8].

To ensure the solution is independent of the number of tracks (in the same sense that a CFD simulation should be grid-independent) over ten thousand droplet tracks are calculated. In order to reduce the computational expense of this large number of tracks interphase sources of momentum, heat and mass transfer are not solved for on a cell-by-cell basis as the track moves through the computational grid, as is the usual practice, rather the residence time and surface area of droplets within a cell are summed. From a knowledge of the mass flow associated with each track, fields of the liquid phase volume fraction and sauter mean diameter can then be derived. These two fields are used to calculate the interphase sources of momentum, heat and mass transfer on a cell-by-cell basis after the Lagrangian calculation has been completed. The volume fraction field also allows cell volume and area porosities to be set so that gas velocities satisfy continuity, i.e. they are based on the actual volume of the top space available for gas flow.

Assumptions are made concerning the initial conditions of each droplet track at the 'bath surface' of the top space model. Normal distributions are assumed for the track velocity and size, and the track trajectory is set so that its initial motion is in the radial direction of the bath plume with which the track is associated. This last assumption is made so as to generate a 'fountain' above each of the bath plumes assumed to be produced from the bottom injection of raw materials. Depending on the arrangement of the bottom injection tuyeres, these 'fountains' will overlap and form a concentrated volume of metal and slag through which the process gases flow.

Given the size range assumed for the droplets and the velocities of the hot air blast, calculations indicate that breakup of the larger droplets is likely[9]. The breakup phenomenon is incorporated into the Lagrangian droplet tracking model where a test on the critical Weber number is made and the droplet size reduced if a breakup event has occurred. The breakup of droplets, especially in the high velocity regions of the post combustion jet, results in increased liquid surface area and thereby a larger amount of heat, mass and momentum transfer between liquid and gas. The production of sub-millimetre droplets within the jet causes the jet to decelerate and spread radially outwards, and the droplets to be turned back along the direction of the jet, as a consequence of increased interphase drag.

The model accounts for the decarburisation of droplets through surface reactions with carbon dioxide and oxygen. These reaction mechanisms introduce further carbon monoxide into the top space, i.e. in addition to that produced by the bottom injection of raw materials. The droplet reaction mechanics occurring within the top space of the HIsmelt vessel have been discussed in detail by Cusack et al[10]. The kinetics of reaction at the droplet surface have to date been considered to be fast

and therefore neglected in the model. On this basis the decarburisation rate is simply controlled by gas boundary layer diffusion. However, when the droplets are small and are located in a high velocity region of the top space, mass transfer will not be rate limiting and reaction kinetics will be important.

2.3 Swirl Tuyere

Since the early days of the HIsmelt technology development considerable effort has been employed in the investigation of various top lance and tuyere configurations used to produce the post combustion jet[11]. Investigation has been made into the use of multi-hole post combustion lances as well as a 'bent tuyere' design. To overcome the shortcomings of the original tuyere designs an adjustable tuyere was designed which could alter the jet shape and hardness through the use of varying degrees of swirl. This design has been successful in producing increased levels of post combustion with only minor deterioration in the heat transfer efficiency.

The turbulence characteristics of a swirling jet are quite different from that of an axisymmetric round jet due to the anisotropic nature of the flow. Because of this it was understood that the standard k-ε model of turbulence, which has been used extensively for other industrial flow problems, would not be appropriate for predicting the turbulence within the post combustion jet. More sophisticated turbulence models could be used for this flow situation such as the algebraic stress model of Boysan and Swithenbank[12], or a Reynolds stress model. However, a simpler solution has been used in which different turbulence models are applied to different momentum equations as suggested by Frith and Duggins[13]. Thus, the k-ε model is used for the axial and radial momentum equations whilst a Prandlt mixing-length model (based on the radial velocity gradient) is used for the swirl momentum equation. In this manner the major diffusion contributions in the momentum equations are handled in a straightforward manner, and the convergence difficulties and computational expense associated with the more sophisticated turbulence models are avoided. It should also be noted that whilst more sophisticated models may give more accurate predictions in the region of the swirling jet, the applicability of any turbulence model within the droplet region of the process is not immediately obvious.

In order to assess the validity of this hybrid turbulence model, physical modelling studies were performed at the CSIRO on a one third scale isothermal model of the tuyere and jet. A CFD model was constructed to simulate the experimental conditions and a comparison made between the experimental data and the flow predictions; this comparison is shown in figure 3. Radial profiles of axial and swirl velocity for two turbulence models are compared with experimental measurements at a downstream distance of 200 mm.

The radiation modelling used within the top space model is based on the polar form of the six-flux model suggested by Hamaker[14] and further developed by other workers[15,16]. This model has been further extended to account for the radiation effects arising from the presence of a particulate phase[17]. In the current implementation the in-depth absorptivity and scattering coefficients of the model are modified according to the local surface area of the droplets.

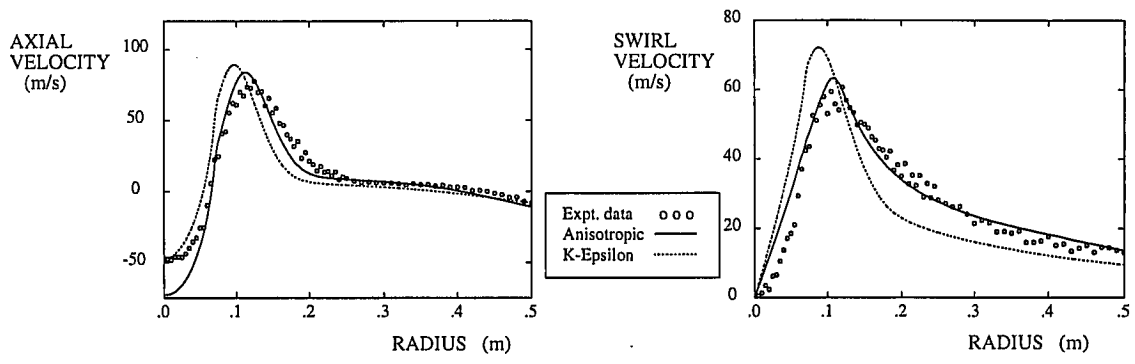

Figure 3. Comparison of measured jet velocities with model predictions.

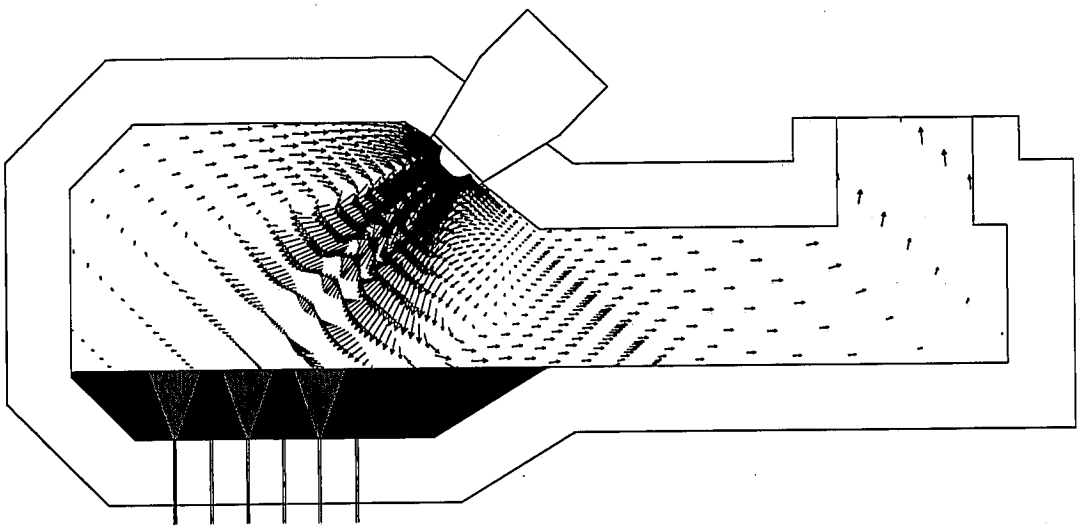

Figure 4. HRDF top space simulation: velocity vectors.

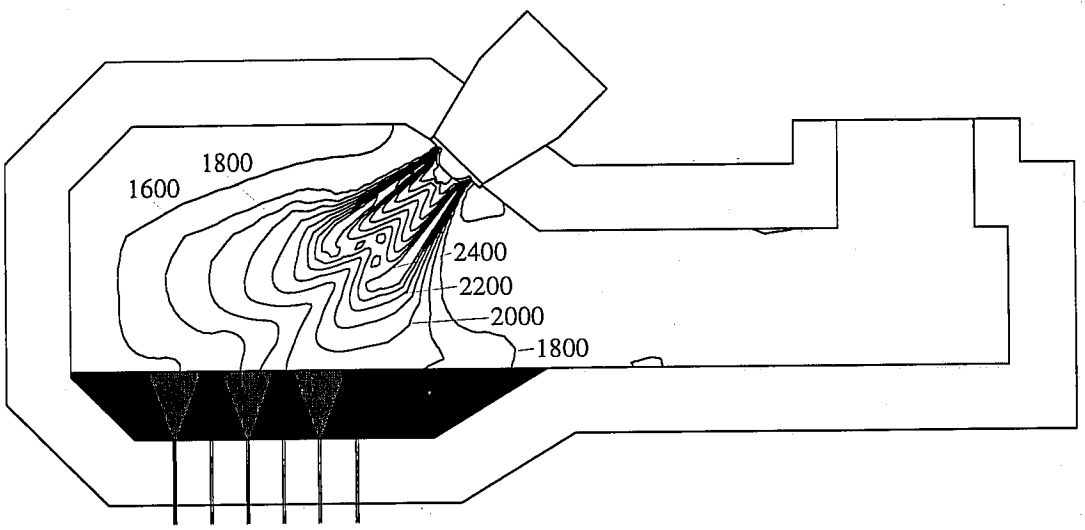

Figure 5. HRDF top space simulation: contours of gas temperature (deg. C).

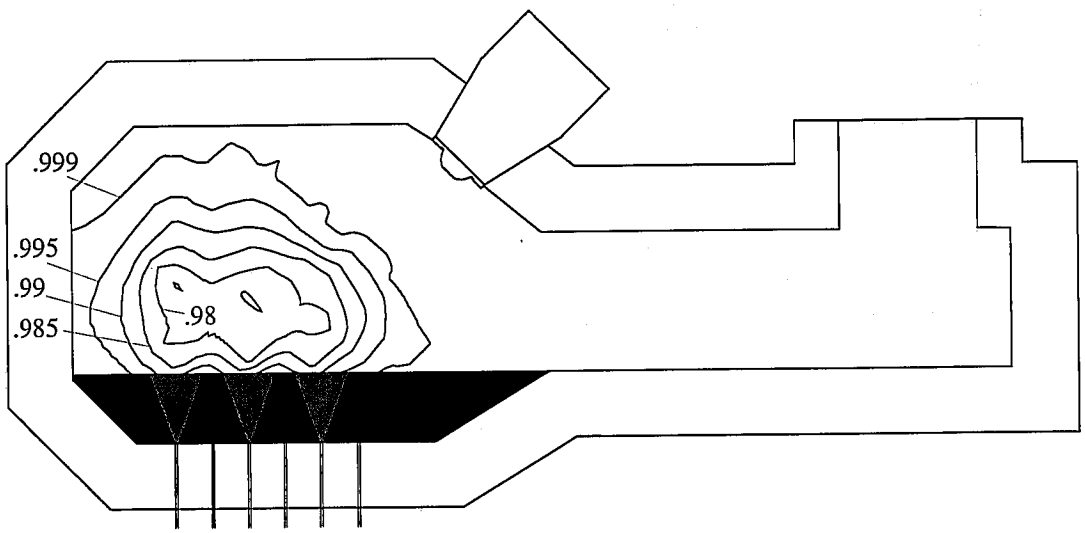

Figure 6. HRDF top space simulation: contours of gas volume fraction.

Figures 4 to 6 show typical predictions from a top space model simulation of the horizontal vessel at the HRDF in Kwinana, Western Australia. These figures show velocity vectors, gas temperature and gas volume fraction for a reduction run in which the post combustion jet has a high degree of swirl.

Figure 4, showing gas velocity vectors, reveals the flow of the hot air blast through the transition zone across the surface of the bath. This flow recirculates back towards the post combustion jet (via the back wall and roof) where it either entrains into the jet or passes around it and on towards the stack. The fineness of the computational grid in the region of the jet can be seen by the high concentration of velocity vectors in this location.

The gas temperature contours of figure 5 reveal the flame front around the jet where the entrained carbon monoxide reacts with jet oxygen to form carbon dioxide. As the gas travels through the transition zone convective heat transfer with the droplets reduces the gas temperature. On the stack side of the jet where the density of droplets is less (refer to figure 6), the gas is not cooled to the same extent.

The droplet populated region of the transition zone is clearly evident in figure 6 which shows contours of gas volume fraction. In this simulation the maximum volume fraction of the liquid phase is located above the middle bath plume and has a value of approximately 2%.

3. BATH MODELLING

So far the paper has highlighted the importance of top space modelling. However, fluid mechanics phenomena within the iron bath are critical to achieving process chemistry objectives and also to engineering aspects of vessel design. Two of the most important engineering considerations are (a) designing appropriate means of introducing coal and ore to the bath (by means of injection) and (b) removing the product from the bath (i.e. tapping). Therefore a large-scale effort has been put into developing a realistic and predictive model of the bath.

The sort of predictions required of the model are:

- The general flow structure within the bath, including delineation of well-mixed and quiescent regions;
- The location of the gas plumes generated by the bottom coal injection and the void fraction within them;
- The mass of droplets contained in the fountain generated by bottom injection and the distribution of that mass through the top-space; and
- The dissolution of coal and the smelting of ore particles within the iron bath.

The information gained from these predictions has many applications, for example:

- The fountain mass distribution is critical in the determination of post combustion and heat transfer efficiency via the top-space model;
- The results can be used to guide the placement of bottom tuyeres;
- The results can be used to guide the placement of tapholes;
- The fountain mass distribution is valuable in designing the vessel so as to minimise carry-over;
- The models provide a "bridge" between physical water models and the real vessels allowing correct interpretation of water model data despite density and temperature differences; and
- The models provide an invaluable tool for scaling up pilot plant results to commercial scale and checking proposed commercial scale designs.

3.1 Mathematical Model of the Bath

The bath dynamics must be considered to be multi-phase, consisting as it does of gas, liquid metal, liquid slag, and particles of coal and ore of various sizes. To treat the main gas and liquid phases, the so-called multi-fluid (or Eulerian-Eulerian) technique has been used. In this method both gas and liquid phases are treated mathematically as continua, with each continuum phase occupying only a fraction of available space - its volume fraction. The volume fraction varies from place to place

depending on the relative amount of that phase present, so that in the top-space the gas fraction is high and in the bath the liquid fraction is usually high. Small-scale structure (e.g. bubbles and droplets) must be smoothed over to allow the equations to be solved in a reasonable time using today's computers. This small-scale structure is however critical to heat, mass and momentum transfer because it determines the interfacial area, so sub-grid models must be used to account for the effect of this fine structure.

The primary equations solved within the multi-fluid model are the conservation equations of mass, momentum, energy and chemical species given earlier, but with the addition of the phase volume fraction multiplier and time dependence. For example the mass conservation equation for each phase can be written:

$$\frac{\partial(R_i\rho_i)}{\partial t} + \nabla(R_i\rho_i\vec{U}_i) = S_{mi}$$
$$\sum_{i=1}^{n} R_i = 1 \qquad (3)$$

The full set of equations can be found in Schwarz[18]. The equations have been solved within a finite-volume method framework using PHOENICS. The multi-fluid aspect of the solution has been treated using the IPSA algorithm.

As mentioned above, sub-models which describe sub-grid scale physics and chemistry are required. Sub-models that have been developed for the HIsmelt bath model include (i) interphase friction; (ii) turbulent interdiffusion of the phases; (iii) Coal devolatilization; (iv) coal dissolution; and (v) ore smelting.

3.2 Validation

Because of the difficulty with taking fluid dynamic measurements within the smelting vessel, most of the fluid flow model validation has been carried out using water baths, supplemented by information from small-scale molten iron and tin bath models[19]. Results from a typical water bath simulation are given in figure 7: it shows a comparison between

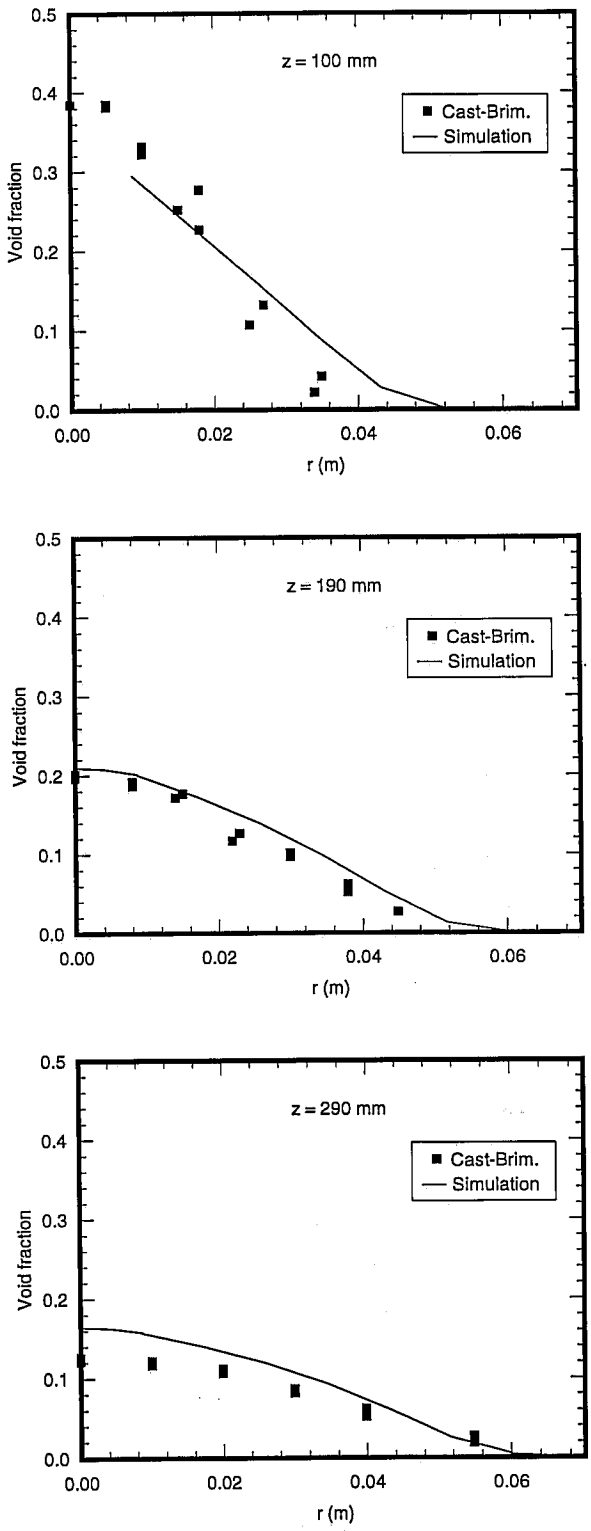

Figure 7. Comparison between predicted and measured profiles of void fraction across a bubble plume.

predicted and measured void fraction in the plume generated by bottom air injection in an experiment by Castillejos and Brimacombe[20]. At each height, the profile of void fraction

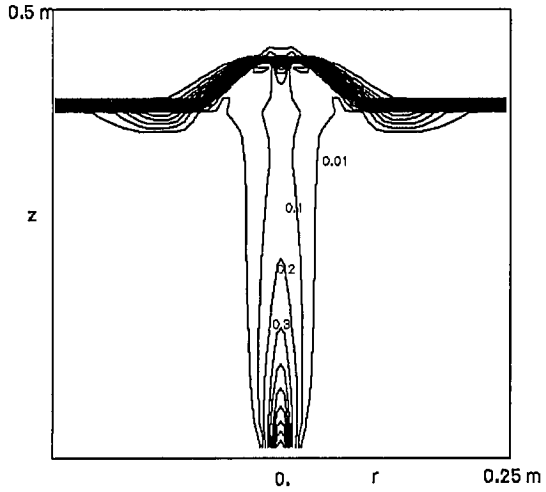

Figure 8. Predicted void fraction contours for a water model of bottom gas injection showing the swelling of the bath surface.

across the plume is in good agreement with the data. Figure 8 shows void fraction contours for a similar experiment, including the swelling of the bath surface where the plume reaches the surface. The height and shape of the swelling is in excellent accord with measurements[21].

3.3 Time-averaged Models

Most of the important features of the bath dynamics can be determined by solving for the time-averaged flow. This modelling approach has the decided advantage that solutions to complex vessels with multiple tuyeres can be obtained in a reasonable amount of computer time, though clearly bath slopping and wave motion cannot be studied. Examples of models of bath motion with a horizontally oriented smelting vessel have been given in Hardie et al[5] and Schwarz[22].

An integral part of the time-averaged flow simulation is the computation of the mass distribution in the top-space of the vessel using a Lagrangian droplet tracking program. This follows the paths of many droplets from the bath surface through the top-space and back to the bath. The predicted droplet distribution has been validated by measuring mass distributions in a full-scale water model of a HIsmelt vessel. Figure 9 shows typical predicted distributions of droplet mass on four cross-sections through a horizontal vessel.

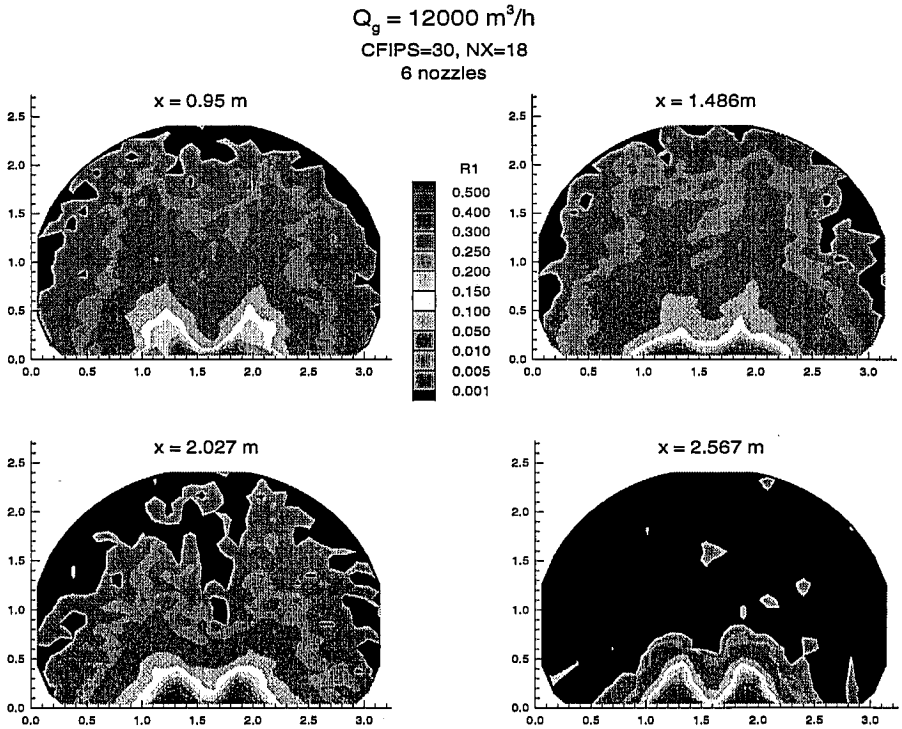

Figure 9. Four cross-sections through a pilot plant SRV showing the predicted distribution of liquid droplets in the fountain.

The fountain of droplets is important to achieving high heat transfer efficiency because it is a primary route for returning radiant and convective heat from the post combustion flame back to the bath.

3.4 Transient Models

An unsteady solution of the multi-fluid equations is extremely expensive computationally for a fully 3D representation of a multi-tuyere smelting vessel. However, it yields more information relating to bath slopping and wave motion, gas-liquid plume oscillation within the bath, and the dynamic motion of the droplet fountain in the top-space.

An example of such a calculation is shown in figure 10 in which four snapshots of the liquid distribution in a possible HIsmelt vessel configuration are given. The vertical section shown through the 3D model of the vessel passes through a tuyere on one side of the vessel and half-way between tuyeres on the other side. The gas-liquid plume is seen to move from side to side and also to pulse semi-periodically. It should be noted that most of the gas passing through the bath is generated in the bath by devolatilization of coal, and a complex interaction between plume dynamics and devolatilization exists.

3.5 Slag-Metal Models

Though the presence of a slag layer in the SRV is not essential to the HIsmelt Process, a slag layer will nonetheless be produced and will have important influences on the bath fluid dynamics and metal quality. A technique has been developed to simulate multiple liquids within the HIsmelt bath, accounting for surface tension and density difference between the liquids. The technique has been validated using experiments on oil-water baths in which entrainment of oil droplets in the underlying water was studied.

Figure 11 illustrates predictions of the technique for an iron bath 0.75 m deep with an overlying slag layer 0.25 m deep within an idealised cylindrical vessel. Gas is injected into the bath at a rate of 200 Nm^3/hr and the figure shows one instant in a transient

Figure 10. Four snapshots at time intervals of 0.3 seconds from a simulation of the liquid distribution inside a possible HIsmelt vessel.

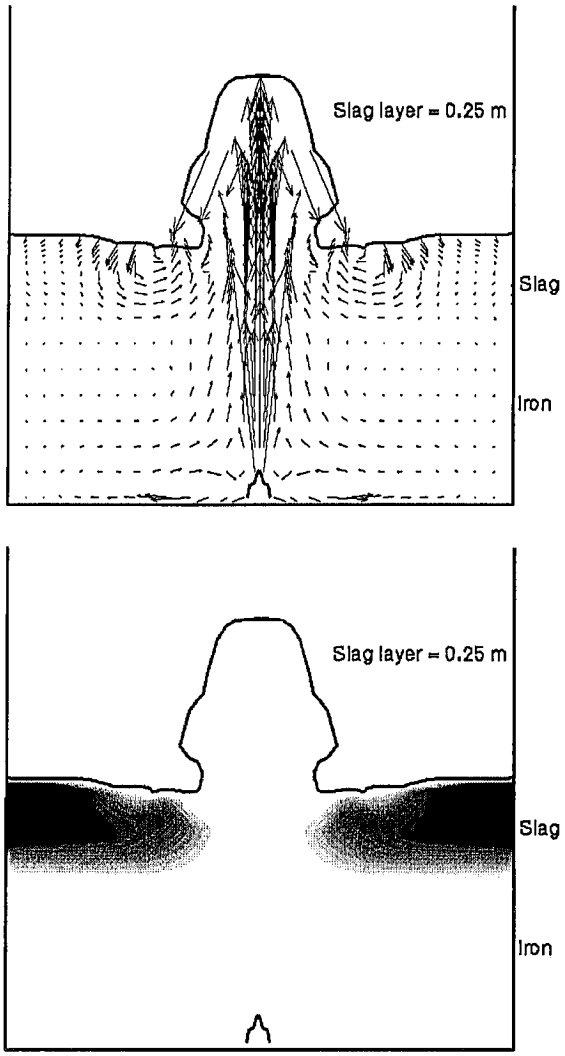

Figure 11. Distribution of slag (bottom) and liquid velocity field (top) at one instant for gas injection into a slag-metal bath. The solid line shows the approximate position of the bath and fountain surface at that instant.

simulation. The slag sits as an annulus around the edge of the vessel, with the gas-liquid plume region reasonably free of slag droplets. The behaviour of the slag layer is quite different from the behaviour of an oil layer on water for the same volumetric gas rate: there is much less entrainment of the lighter fluid down into the heavier fluid in the case of slag compared with the oil case. This is a result of the higher relative density difference for slag-iron and the higher interfacial tension which reduces the tendency of the lighter liquid to break into small droplets. The flow field is different from that found for lower gas flow-rates (e.g. in ladle metallurgy applications) because the gas-liquid plume penetrates the slag layer; metal flow is not deflected onto a path along the base of the slag layer as occurs with lower rates.

4. FUTURE CONSIDERATIONS

The aerodynamics of the top space play a crucial role in the efficiency of the HIsmelt Process. CFD predictions must be accurate enough to reflect this importance. Many factors affect accuracy, some of which are due to uncertainties in the mathematical representation of the physics involved (turbulence being the prime example), some which relate to the accuracy of the numerical approximations introduced in discretising the original transport equations, and some that are to do with geometrical approximations of the real SRV. The final two factors are heavily influenced by the grid used. Good grid design for a finite-volume solution requires that, as far as it is possible, the mesh is orthogonal, that mesh lines are either parallel or perpendicular to solid boundaries and, most importantly, that the mesh is aligned with the dominant flow direction. There are high order numerical schemes that help to remove or moderate some of these factors, but are applicable only to simpler flow situations.

Flow in the SRV is mainly governed by the post combustion jet(s) which operate at near sonic conditions. The mesh is therefore aligned with the jet axis and, if the flow is swirling, the polar form of the equations is used to provide the best characteristics for the tangential velocity component. However, as the HIsmelt Process increases in scale to a full-size production facility, the need to add multiple air tuyeres becomes apparent. It is then necessary to resort to unstructured meshes so that alignment of the mesh with each jet is retained; as a bonus a better alignment with the vessel walls can also be obtained. The unstructured mesh finite-volume code PHYSICA[23] has been used for this purpose. The mesh required for a two-tuyere horizontal vessel is shown in figure 12. Two polar sections follow the inclination of the jets. Iterative adjustment of cell corners of the original mesh (created by a standard FE mesh generator) improves orthogonality near the walls.

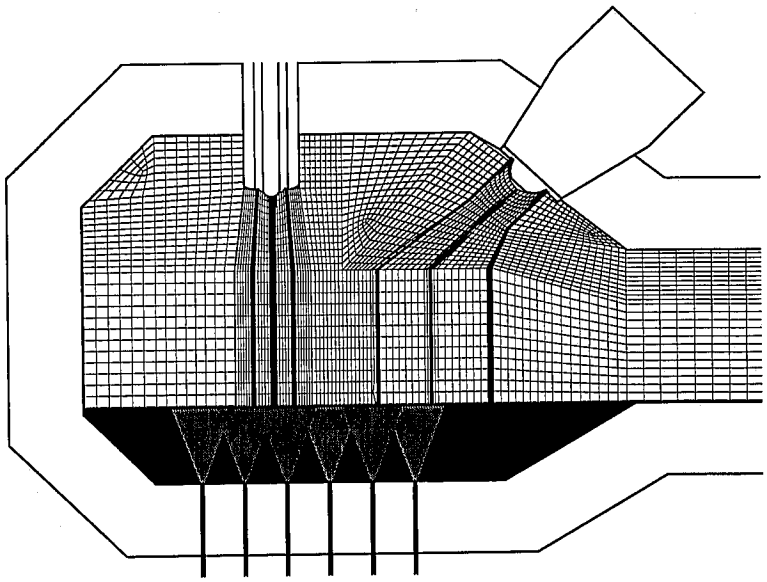

Figure 12. Twin-tuyere SRV with an unstructured mesh.

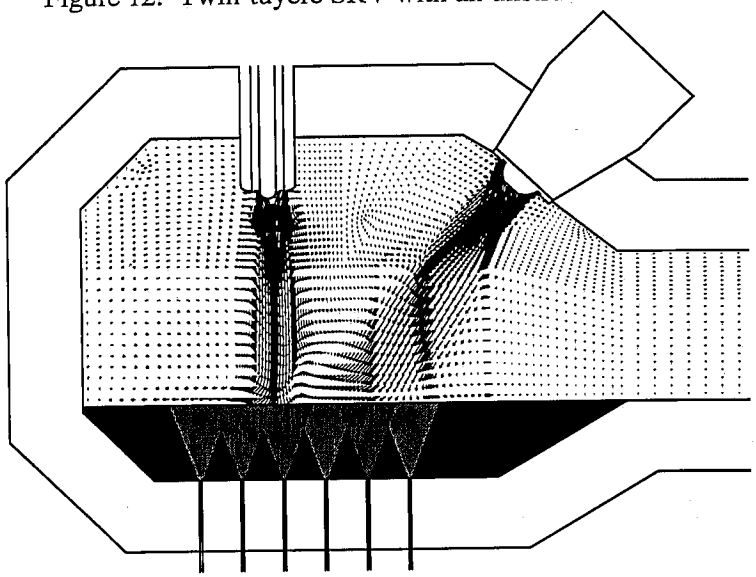

Figure 13. Twin-tuyere SRV velocity field.

Preliminary results obtained for this case, for isothermal conditions and without a transition zone, are shown in figure 13. The velocity vectors indicate a strong interaction between the jets and in particular the structure at their intersection.

In terms of the physics of the model more sophisticated droplet breakup models exist, which can account, for example, for the time delay between a drop encountering a shear layer and its eventual break up[24]. These developments will accompany more detailed treatment of the droplet chemistry to account, for example, for the possibility of carbon depletion.

In the long term, emerging numerical techniques will enable finer meshes to be used and parallel computers will enable full coupling between the bath and top space models leading to a better description of the dynamics of the process. Other more exotic possibilities include the introduction of thermal stress computations in the model to compute refractory wear caused by thermal transients, due to successive irradiation and bath washing of the brick surface.

5. CONCLUDING REMARKS

The HIsmelt Process has been a fertile ground for new ideas in the CFD modelling of a very complex industrial process. The close coupling of plant experiments and CFD simulations happened at a time when CFD was still emerging as a potent but still unproven design tool. The faith shown in its potential has paid off, in the way that many intermediate designs of the SRV were quickly evaluated before any metal was cut. In addition the benefits of greater understanding of this new high intensity process through this detailed mathematical modelling, although not easily quantifiable, cannot be underestimated.

The model is still developing and it still has deficiencies in some areas, especially where the physics are not well understood. However, the epilogue must be, that even with these deficiencies, the HIsmelt Process would not have reached the stage it is now at, in the space of fourteen years, without the help of CFD simulations.

ACKNOWLEDGMENTS

The modelling work described in this paper has come about through the enthusiastic contributions of many colleagues associated with the development of the HIsmelt Process. It is a pleasure to acknowledge the contributions of Greg Hardie and Peter Burke (HIsmelt), Robin Batterham and Gary Brown (CRA), Nick Croft (Greenwich University), and the experimental work of John Hooper and Tony Musgrove (CSIRO).

Others who have made important contributions to the work reported here include various CSIRO, CHAM, and Greenwich University colleagues.

REFERENCES

1. Brotzmann, K., 1987, "New Concepts and Methods for Iron and Steel Production," *Steelmaking Conference Proceedings, ISS-AIME*, **70**, pp. 3-12.

2. Innes, J.A. Moodie, J.P. Webb, I.D. and Brotzmann, K., 1988, "Direct smelting of Iron Ore in a Liquid Iron Bath, the HIsmelt Process," *Process Technology Conference Proceedings, ISS-AIME*, **7**, pp. 225-231.

3. Innes, J.A. Cusack, B.L. Batterham, R.J. Hardie, G.J. and Burke, P.D., 1991, "The HIsmelt Process: Adding value to Australia's Mineral Resources," *Proceedings CHEMECA '92.*

4. Keogh, J.V. Hardie, G.J. Philp, D.K. and Burke, P.D., 1991, "HIsmelt Process Advances to 100,000 t/y plant," *Ironmaking Conference Proceedings, ISS-AIME*, **50**, pp. 635-649.

5. Hardie, G.J. Cross, M. Batterham, R.J. Davis, M.P. and Schwarz, M.P., 1992, "The Role of Mathematical Modelling in the Development of the HIsmelt Process," *10th Process Technology Conference Proceedings, ISS-AIME*, pp. 109-121.

6. Moodie, J.P. Davis, M.P. and Cross, M., 1988, "Numerical Modelling for the Analysis of Direct Smelting Processes," *7th Process Technology Conference Proceedings, ISS-AIME*, pp. 55-64.

7. Clift, R. and Gauvin, W.H., 1970, "Proceedings of *CHEMECA* '70," **1**, pp. 14-28.

8. Rowe, P.N. Claxton, K.T. and Lewis, J.B., 1965, "Heat and Mass Transfer from a Single Sphere in an Extensive Flowing Fluid," *Trans. Inst. Chem. Eng.*, **41.**

9. Clift, R. Grace, J.R. and Weber, M.E., 1978, "Formation and Breakup of Fluid Particles," *Bubbles Drops and Particles,* Academic Press, London, pp. 339-346.

10. Cusack, B.L. Hardie, G.J. and Burke, P.D., 1991, "HIsmelt - 2nd Generation Direct Smelting," *Second European Ironmaking Conference*, Glasgow.

11. Hardie, G.J. Taylor, I.F. Ganser, J.M. Wright, J.K. Davis, M.P. and Boon, C.W., 1992, "Adaptation of Injection Technology for the HIsmelt Process," *Proc. Savard/Lee International*

Symposium on Bath Smelting, Ed. J.K. Brimacombe et al., TMS, pp. 623-644.

12. Boysan, F. Ayers, H. and Swithenbank, J., 1982, "A fundamental Mathematical Modelling Approach to Cyclone Design," *Trans IChemE*, **60**.

13. Frith, P.W.C. and Duggins, R.K., 1985, "Turbulence Modelling of Swirling Flows," *Numerical Methods in Laminar and Turbulent Flow*, Ed. Taylor et. al., Pineridge Press, Swansea, pp. 353-363.

14. Hamaker, H.C., 1947, "Radiation and Heat Conduction in Light Scattering Material," *Philips Research Reports*, 2, 55, 103, 112, and 420.

15. Lockwood, F.C. and Shah, N.G., 1978, "Evaluation of an Efficient Radiation Flux Model for Furnace Prediction Procedure," *Sixth International Heat Transfer Conference*.

16. Varnas, S.R. and Truelove, J.S., 1995, "Simulating Radiative Transfer in Flash Smelting Furnaces," *Appl. Math. Modelling*, **19**.

17. Kostamis, P., 1987, "Computer modelling and analysis of particulate laden flows," *PhD Thesis*, University of Greenwich.

18. Schwarz, M.P., 1996, "Simulation of Gas Injection into Liquid Melts," *Applied Math. Modelling*, **20**, pp. 41-51.

19. Schwarz, M.P. and Dang, P., 1995, "Simulation of Blowthrough in Smelting Baths with Bottom Injection," *Proceedings of the 13th Process Technology Division Conference, ISS-AIME*, pp. 415-422.

20. Casillejos, A.H. and Brimacombe, J.K., 1987, "Measurement of Physical Characteristics of Bubbles in Gas-Liquid Plumes: Part 1 An Improved Electroresistivity Probe Technique," *Metall. Trans. B*, **18B**, pp. 659-671.

21. Sahajwalla, V. Casillejos, A.H. and Brimacombe, J.K., 1990, "The Spout of Air Jets Upwardly Injected into a Water Bath," *Metall. Trans. B*, **21B**, pp. 71-80.

22. Schwarz, M.P., 1994, "The Role of Computational Fluid Dynamics in Process Modelling," *6th AusIMM Extractive Metallurgy Conference*, pp. 31-36.

23. PHYSICA, 1996, University of Greenwich, London.

24. Kolev, N.I., 1993, "Fragmentation and Coalescence Dynamics in Multiphase Flows," *Experimental Thermal and Fluid Science*, **6**, pp. 211-251.